Thin film MoS$_2$ nanocrystal based ultraviolet photodetector

S. Alkis,[1,2] T. Öztaş,[1] L. E. Aygün,[1,2] F. Bozkurt,[1,2] A. K. Okyay,[1,2,3] and B. Ortaç[1*]

[1]*Institute of Material Science and Nanotechnology (UNAM), Bilkent University, 06800, Bilkent, Ankara, Turkey*
[2]*Department of Electrical and Electronics Engineering, Bilkent University, 06800, Bilkent, Ankara, Turkey*
[3]*aokyay@ee.bilkent.edu.tr*
[*]*ortac@unam.bilkent.edu.tr*

Abstract: We report on the development of UV range photodetector based on molybdenum disulfide nanocrystals (MoS$_2$-NCs). The inorganic MoS$_2$-NCs are produced by pulsed laser ablation technique in deionized water and the colloidal MoS$_2$-NCs are characterized by transmission electron microscopy, Raman spectroscopy, X-ray diffraction and UV/VIS absorption measurements. The photoresponse studies indicate that the fabricated MoS$_2$-NCs photodetector (MoS$_2$-NCs PD) operates well within 300-400 nm UV range, with diminishing response at visible wavelengths, due to the MoS$_2$-NCs absorption characteristics. The structural and the optical properties of laser generated MoS$_2$-NCs suggest promising applications in the field of photonics and optoelectronics.

©2012 Optical Society of America

OCIS codes: (230.5160) Photodetectors (310.0310) Thin films; (350.3390) Laser materials processing.

References and links

1. H. Qiu, L. Pan, Z. Yao, J. Li, Y. Shi, and X. Wang, "Electrical characterization of back-gated bi-layer MoS$_2$ field-effect transistors and the effect of ambient on their performances," Appl. Phys. Lett. **100**(12), 123104 (2012).
2. B. Radisavljevic, A. Radenovic, J. Brivio, V. Giacometti, and A. Kis, "Single-layer MoS$_2$ transistors," Nat. Nanotechnol. **6**(3), 147–150 (2011).
3. Q. Li, J. T. Newberg, E. C. Walther, J. C. Hemminger, and R. M. Penner, "Polycrystalline molybdenum disulfide (2H-MoS$_2$) nano- and microribbons by electrochemical/chemical synthesis," Nano Lett. **4**(2), 277–281 (2004).
4. M. Shanmugam, T. Bansal, C. A. Durcan, and B. Yu, "Molybdenum disulfide/ titanium dioxide nanocomposite-poly 3-hexylthiophene bulk heterojunction solar cell," Appl. Phys. Lett. **100**(15), 153901 (2012).
5. Y. Yoon, K. Ganapathi, and S. Salahuddin, "How good can monolayer MoS$_2$ transistors be?" Nano Lett. **11**(9), 3768–3773 (2011).
6. S. Ross and A. Sussman, "Surface oxidation of molybdenum disulfide," J. Phys. Chem. **59**(9), 889–892 (1955).
7. Z. Yin, H. Li, H. Li, L. Jiang, Y. Shi, Y. Sun, G. Lu, Q. Zhang, X. Chen, and H. Zhang, "Single-layer MoS$_2$ phototransistors," ACS Nano **6**(1), 74–80 (2012).
8. R. Tenne, L. Margulis, M. Genut, and G. Hodes, "Polyhedral and cylindirical structures of tungsten disulphide," Nature **360**(6403), 444–446 (1992).
9. M. Redlich, A. Katz, L. Rapoport, H. D. Wagner, Y. Feldman, and R. Tenne, "Improved orthodontic stainless steel wires coated with inorganic fullerene-like nanoparticles of WS$_2$ impregnated in electroless nickel-phosphorous film," Dent. Mater. **24**(12), 1640–1646 (2008).
10. C. L. Stender, E. C. Greyson, Y. Babayan, and T. W. Odom, "Patterned MoS$_2$ nanostructures over-centimeter square areas," Adv. Mater. (Deerfield Beach Fla.) **17**(23), 2837–2841 (2005).
11. H. Wu, R. Yang, B. Song, Q. Han, J. Li, Y. Zhang, Y. Fang, R. Tenne, and C. Wang, "Biocompatible inorganic fullerene-like molybdenum disulfide nanoparticles produced by pulsed laser ablation in water," ACS Nano **5**(2), 1276–1281 (2011).
12. M. Nath and C. N. R. Rao, "Nanotubes of group 4 metal disulfides," Angew. Chem. **114**(18), 3601–3604 (2002).
13. G. R. Samarodnitzky-Naveh, M. Redlich, L. Rapoport, Y. Feldman, and R. Tenne, " Inorganic fullerene-like tungsten disulfide nanocoating for friction reduction of nickel–titanium alloys," Nanomedicine **4**, 943–950 (2009).
14. H. Liu and P. D. Ye, "MoS$_2$ nanoribbon transistors: Transition from depletion mode to enhancement mode by channel-width trimming," IEEE Electron Device Lett. **33**, 546–548 (2012).
15. E. Gourmelon, O. Lignier, H. Hodouda, G. Couturier, J. C. Bernede, J. Tedd, J. Pouzet, and J. Salardenne, "MS$_2$ (M=W, Mo) photosensitive thin films for solar cells," Sol. Energy Mater. Sol. Cells **46**(2), 115–121 (1997).

16. J. N. Coleman, M. Lotya, A. O'Neill, S. D. Bergin, P. J. King, U. Khan, K. Young, A. Gaucher, S. De, R. J. Smith, I. V. Shvets, S. K. Arora, G. Stanton, H. Y. Kim, K. Lee, G. T. Kim, G. S. Duesberg, T. Hallam, J. J. Boland, J. J. Wang, J. F. Donegan, J. C. Grunlan, G. Moriarty, A. Shmeliov, R. J. Nicholls, J. M. Perkins, E. M. Grieveson, K. Theuwissen, D. W. McComb, P. D. Nellist, and V. Nicolosi, "Two-dimensional nanosheets produced by liquid exfoliation of layered materials," Science **331**(6017), 568–571 (2011).
17. Y. Zhan, Z. Liu, S. Najmaei, P. M. Ajayan, and J. Lou, "Large-area vapor-phase growth and characterization of MoS$_2$ atomic layers on a SiO$_2$ substrate," Small **8**(7), 966–971 (2012).
18. C. M. Zelenski and P. K. Dorhout, "Templete synthesis of near-monodisperse microscale nanofibers and nanotubes of MoS$_2$," J. Am. Chem. Soc. **120**(4), 734–742 (1998).
19. W. K. Hsu, B. H. Chang, Y. Q. Zhu, W. Q. Han, H. Terrones, M. Terrones, N. Grobert, A. K. Cheetham, H. W. Kroto, and D. R. M. Walton, "An alternative route to molybdenum disulfide nanotubes," J. Am. Chem. Soc. **122**(41), 10155–10158 (2000).

1. Introduction

Semiconductor nanocrystals have been under intense investigation for the past decade due to the potential applications in new nanomaterials based devices. MoS$_2$ is a newly emerging transition-metal dichalcogenide (TMD) semiconductor material which is rallied up as finite-energy-bandgap alternative to graphene in advanced electronic and photonic device applications [1, 2]. The presence of its natural bandgap (~1.2 eV indirect bandgap in multilayer/bulk form, ~1.85 eV direct bandgap in monolayer form) makes it advantageous compared to graphene-based CMOS-like logic device applications [1, 5]. It is also shown that MoS$_2$ TMDs resist oxidation in moist air environments at temperatures up to 85°C which makes them more durable in device fabrication compared to Silicon and Germanium nanostructures [3, 6]. Si-based transistors are outperformed at the scaling limit by TMDs owing to the absence of dangling bonds and low dimensionality [1, 5].

Due to their 2D ultra-thin atomic layer structure, MoS$_2$/WS$_2$ TMDs are shown to exhibit unique physical, optical and electrical properties [4, 7]. Their fullerene like nature [8] and their excellent mechanical properties such as friction-reduction and self-lubrication [9] along with their unique optoelectronic properties (UV light absorption [10], band-gap tunability [1, 2]) make MoS$_2$/WS$_2$ nanostructures applicable in heterogeneous catalysis, hydrogen storage, lithium-magnesium ion batteries [11, 12], various bio-medical applications [9, 11, 13] and as well as, various electronic and optoelectronic device applications (transistor, photo-transistor and solar cell applications) [2, 7, 4]. Since they possess interesting optoelectonic properties that are tunable by physical layer thickness, various electronic and photonic devices are fabricated based on MoS$_2$ TMDs, such as hybrid bulk heterojunction solar cells (BHJs) [4], single-layer transistors [2], single-layer phototransistors [7] and back-gated bi-layer field-effect transistors [1]. Despite the fact that, single-layer MoS$_2$ has a large direct bandgap of 1.8 eV and a low electron mobility of 0.5-3 cm^{2}V^{-1}s^{-1}, Radisavljevic et al. showed that, in a single-layer transistor based on MoS$_2$ TMDs, it is possible to achieve an electron mobility of 200 cm^{2}V^{-1}s^{-1} and an on/off ratio of 10^8 using hafnium oxide gate dielectric material [2]. This work has been very good indicator of MoS$_2$ TMDs potential to complement graphene in electronics applications [2]. Recently, Liu et al. showed that, for MoS$_2$ TMD based transistors, it is further possible to achieve an electron mobility of 517 cm^{2}V^{-1}s^{-1} using a multilayer MoS$_2$ flake as the channel material [14], compared to the single-layer one used by Radisavljevic [2]. In addition to transistor applications, it is shown in the literature that, MoS$_2$ TMDs are also potential candidates in solar cell applications [4, 15]. In 1997 Gourmelon et al. came up with the idea of using MoS$_2$ thin films in solar cell applications [15] and later on, Shanmugam et al. fabricated a hybrid bulk heterojunction (BHJ) solar cell based on MoS$_2$/TiO$_2$ nanocomposites and showed that MoS$_2$ TMDs are also applicable in solar cell applications [4]. All these research results demonstrate the great potential that MoS$_2$ TMDs have in terms of nanoelectronics and nanophotonics applications.

There are various ways of synthesizing MoS$_2$ TMD nanostructures including solution-based exfoliation [16], CVD based synthesis [17], thermal decomposition [18], powder sublimation [19] and electrochemical/chemical synthesis [3]. Another promising method for

obtaining MoS_2 TMD nanostructures is the laser ablation method [11]. Laser ablation is a versatile nanoparticle synthesis technique which can be applied at industrial scales. However, there are very limited reports on the applications of MoS_2-NCs synthesized by laser ablation. Wu et al showed that MoS_2 TMD nanoparticles that are obtained through laser ablation are fullerene-like and have good solubility and biocompatible nature which opens the doors for MoS_2 TMD nanostructure applications in various biomedical areas [11].

Here, we present for the first time the development of UV photodetector based on MoS_2-NCs. The pulsed laser ablation technique in deionized water allows generating crystalline inorganic MoS_2-NCs. The colloidal MoS_2-NCs were characterized by transmission electron microscopy, X-ray diffraction and UV/VIS absorption measurements. The photocurrent measurements demonstrate that the fabricated MoS_2-NCs PD operates in UV range from 300 to 400 nm with diminishing response at the visible range.

2. Experiments and results

Colloidal MoS_2-NCs solution was generated by using pulsed laser ablation technique in deionized water using bulk MoS_2 powder (99,99% Sigma-Aldrich). The commercial nanosecond pulsed ND:YLF laser (Empower Q-Switched Laser, Spectra Physics) operated at 527 nm with pulse duration of 100 ns, average output power of 16 W at a pulse repetition rate of 1 kHz corresponding to a pulse energy of 16 mJ were used. The laser beam was focused on the bulk MoS_2 powder target placed in a glass vial containing 10 ml of deionized water using a plano-convex lens with a focal length of 50 mm. The height of liquids layer over the bulk MoS_2 powder target was about 5 mm. The pulsed laser ablation process was carried out for 60 min. To obtain colloidal MoS_2-NCs solution, the solution was continuously stirred by a magnetic stirrer at 800 rpm. MoS_2-NCs PD fabrication was performed on highly p-type (10-18 mohm-cm Boron doped) Si substrate. The substrate was cleaned through standard solvent degreasing and cleaning procedures involving acetone, isopropanol and deionized water. A germanium wetting layer (3nm) followed by 25-nm-thick Ag film was thermally evaporated (VAKSIS-MIDAS) on Si substrate. This was followed by deposition of 5 nm Al_2O_3 (trimethylaluminum and H_2O as the precursor gases 50 cycles at 250°C) on the Ag film by atomic layer deposition (ALD Cambridge Nanotech Savannah 100). Colloidal MoS_2-NCs solution was initially treated in a Branson 2510 type ultrasonic bath with an operating frequency of 40 kHz. In order to form a thin film of MoS_2-NCs on top of the Al_2O_3/Ag/Ge/Si stack, 1.2 grams of polyvinyl alcohol was added to a 20 ml MoS_2-NCs/deionized water solution that was prepared through laser ablation. The solution was stirred vigorously at 90°C for 48 hours in order to dissolve the added polymer and obtain homogeneous solution. The sample surface was then coated with the prepared MoS_2-NCs solution using dip-coating method. This procedure was followed by a second atomic layer deposition of 5 nm Al_2O_3 on top of MoS_2-NCs/Al_2O_3/Ag/Ge/Si structure using the same ALD recipe. 100-nm-thick Ag was evaporated to form the top and bottom electrical contact pads. An Al layer was used for efficient photo-carrier collection and was kept very thin (<10 nm) to allow for light penetration. As supporting information, we should add the transmission vs wavelength for 10 nm Aluminum layer. Illustration of the device structure and an SEM image of a completed photodetector is shown in Fig. 3. The morphology of bulk MoS_2 powder and MoS_2-NCs were performed by using a FEI-Quanta 200 FEG SEM instrument at an accelerating voltage of 20 kV. The morphology and the elemental analysis of the MoS_2-NCs were performed by using a FEI - Tecnai G^2F30 TEM instrument. The optical absorption spectra of the colloidal MoS_2-NCs solution were obtained with a Varian Cary 5000 UV/Vis/NIR spectrophotometer. Raman spectrum of the MoS_2-NCs was performed by Witec Alpha 300S Micro Raman spectrometer with an excitation wavelength of 532 nm (laser power: 10 mW).

We first present the synthesis of colloidal MoS_2-NCs in deionized water. 1 mg of 2H-MoS_2 powder was used as starting material. The powder was first added to 10 ml of deionized water. During the laser ablation process, the formation of colloidal nanoparticle solution

(CNS) in liquid media was observed. In order to obtain well-dispersed nanoparticles solution, the CNS was followed by ultrasonic post-treatment for 100 minutes. The color of the final CNS product became light-orange. To further understand and better characterize the structure and the composition of MoS_2 nanoparticles, detailed scanning transmission electron microscope (STEM) study was performed with High-Angle Annular Dark Field (HAADF). Representative TEM images of the CNS containing MoS_2 nanoparticles obtained by nanosecond pulsed laser ablation are shown in Fig. 1(a) and Fig. 1(b). The images show that nanosecond pulsed laser ablation of a bulk MoS_2 powder target and then ultrasonic treatment of product produced sub-50 nm sized spherical MoS_2 nanoparticles in deionized water. The elemental compositions of the MoS_2 nanoparticles (the inset of Fig. 1(a)) were obtained by EDAX analysis. The peaks related to carbon (C), oxygen (O) and copper (Cu) are associated with the TEM grid used. The presence of the Mo and S peak in the EDAX spectrum confirms that MoS_2 nanoparticles were successfully generated by laser ablation technique with no significant impurities observed. The nanocrystal size distribution is given in the inset of Fig. 1(b). Nanocrystal sizes range from 4.5 nm to 50 nm and most of the nanocrystals are within 10 nm-25 nm range.
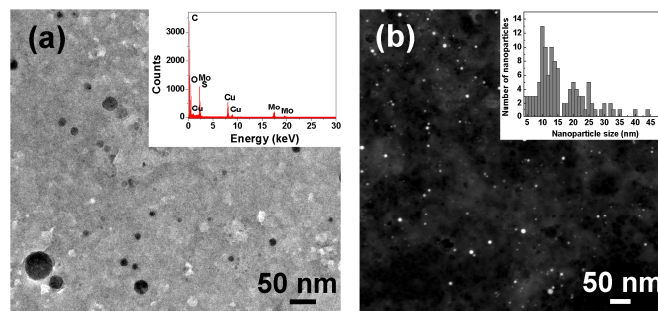

Fig. 1. (a) Representative TEM image of MoS_2-NCs after ultrasonic treatment and the EDAX spectrum in the inset, (b) representative STEM HAADF image of ultrasonic-treated MoS_2-NCs and the size histogram in the inset.

The optical properties of MoS_2-NCs have been characterized by UV/VIS absorption spectroscopy technique. Figure 2(a) shows the normalized optical absorption spectrum of MoS_2-NCs. The optical absorption spectrum of MoS_2-NCs shows a minimum optical absorption feature at 500 nm, strong rising absorption edge shifts towards UV region. The Raman spectrum of MoS_2-NCs given in Fig. 2(b) shows two sharp peaks centered at 381.7 cm^{-1} and 407.5 cm^{-1}. These are attributed to the in-plane E^1_{2g} and out-of-plane A_{1g} vibration of MoS_2-NCs, respectively [11], providing further evidence that the obtained nanocrystals are MoS_2-NCs.
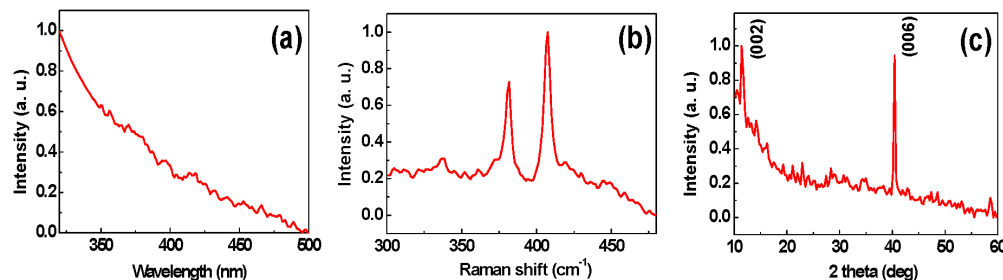

Fig. 2. UV-Vis absorption spectrum of ultrasonic-treated MoS_2-NCs in deionized water (a), Raman spectra of MoS_2-NCs (b), XRD profile of MoS_2-NCs (c).

XRD measurements analyses were also carried out to determine the crystalline structure and the composition of MoS_2-NCs. XRD pattern of ultrasonic-treated MoS_2 NCs is shown in Fig. 2(c). Two main sharp and narrow diffraction peaks at 11.45° (002) and 40.46° (006) are observed. Results indicate that good quality MoS_2-NCs with hexagonal structure were successfully generated by laser ablation technique with no significant impurities [11].

The diagram, SEM image, the electrical and photoresponsivity measurements of the fabricated MoS_2-NCs PD based on MoS_2-NCs obtained through laser ablation are given as in the following. Figure 3(a) shows an illustration of the fabricated MoS_2-NCs PD and Fig. 3(b) shows a top-view SEM image of a completed MoS_2-NCs PD. Figure 4(a) plots electrical current-voltage measurements exhibiting a characteristic exponentially increasing current with applied voltage typical of an insulator-semiconductor-insulator device. We have observed very low dark current density of 3.9 µA/cm^2 at 10V bias from the fabricated MoS_2-NCs PD limited by tunneling through the insulator layers.
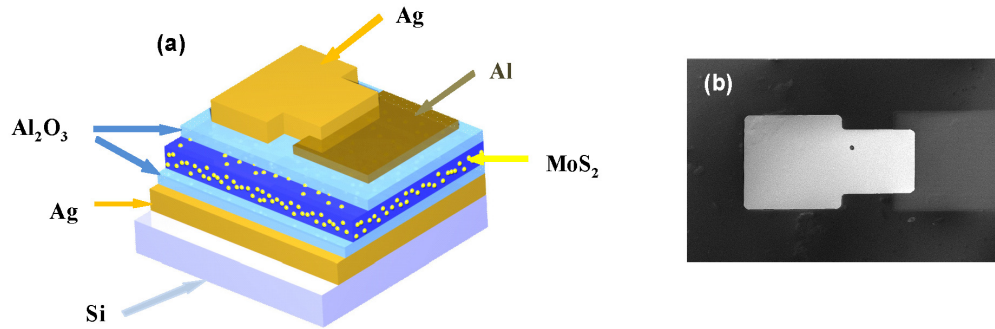

Fig. 3. Diagram of the fabricated MoS_2-NC PD (a) and SEM image of top view of the fabricated MoS_2-NC PD (b).

Photogenerated current (I_{photo}) is measured with mechanically chopped, monochromated white light source (1/8m grating 600 lines/mm) and a lock in amplifier (SRS 830). The optical beam is normally incident on the device as shown in Fig. 3(a). Incident light power (P_{in}) is recorded with a calibrated Silicon photodetector. Spectral responsivity is calculated as the ratio of measuret I_{photo} to P_{in} at each wavelength. Figure 4(b) plots measured relative responsivity vs wavelength of the photodetector. The responsivity at 340 nm illumination is 2.5 times that of 400 nm which agrees well with measured MoS_2-NCs absorption characteristics (Fig. 2(a)).
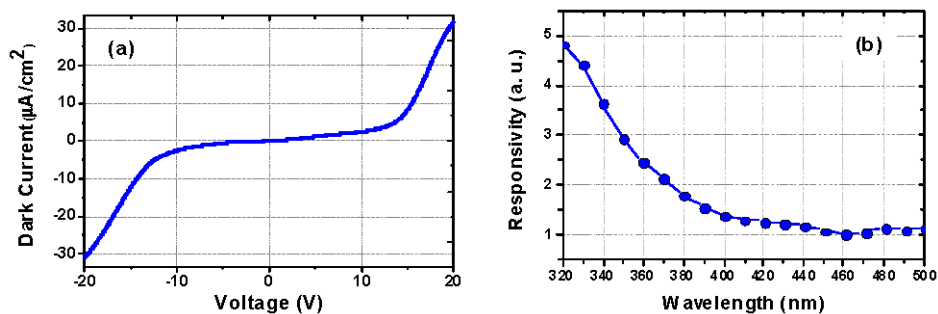

Fig. 4. Dark current-voltage measurements for the fabricated MoS_2-NCs PD (a) and the photoresponsivity vs wavelength data (b).

3. Conclusion

MoS_2-NCs have been obtained through laser ablation in liquid and we have demonstrated that thin film of MoS_2-NCs that have been obtained through laser ablation could be used as a

material for the fabrication of ultraviolet photodetectors. The synthesized MoS_2-NCs gave characteristic Raman peaks at 381.7 cm^{-1} and 407.5 cm^{-1} that are attributed to the in-plane E^1_{2g} and out-of-plane A_{1g} vibration modes of MoS_2 and the crystals gave strong UV absorption towards the UV region. The fabricated MoS_2-NCs PD gave a dark current value of 3.9 $\mu A/cm^2$ under 10 V external bias and the fabricated MoS_2-NCs PD generated photoresponse between 300 to 400 nm UV range and diminishing photoresponse at the visible range. A good agreement is observed between the MoS_2-NCs absorption characteristics and the photoresponsivity data. We beleive that our demonstration will open way to using MoS_2-NCs in new optoelectonic device applications. Photodetectors that are fabricated based on such MoS_2-NCs could offer new advantages over Silicon and Germanium based photodetectors due to the low oxidation tendency of MoS_2-NCs [3, 6].

Acknowledgments